Chinese Journal of Polymer Science Vol. 35, No. 7, (2017), 823–836

Chinese Journal of Polymer Science

Synthesis and Properties of Hydroxide Conductive Polymers Carrying Dense Aromatic Side-chain Quaternary Ammonium Groups*

Guang-hui Nie, Wen-jun Wu, Xi Yue, Shi-jun Liao and Xiu-hua Li **

School of Chemistry & Chemical Engineering, South China University of Technology, Guangzhou 510641, China
The Key Laboratory of Fuel Cell Technology of Guangdong Province, South China University of Technology, Guangzhou 510641, China

Abstract A series of hydroxide conductive polymers QTBMs carrying dense aromatic side-chain quaternary ammonium groups has been synthesized by using a new monomer of 3,3′-di(3″,5″-dimethylphenyl)-4,4′-difluorodiphenyl sulfone and other commercial monomers *via* polycondensation reaction, and subsequent bromination, quaternization and alkalization. The chemical structures of the ionomers were confirmed by ^{1}H- and ^{13}C-NMR spectroscopy. Water uptake, swelling ratio, hydroxide conductivity, the number of bonded water per ammonium group (λ), volumetric ion exchange capacity (IEC_{Vwet}), mechanical and thermal properties, and chemical stability were systematically evaluated for the series of QTBMs membranes. QTBMs showed IECs ranging from 1.02 meq·g^{-1} to 2.11 meq·g^{-1}; in particular, QTBM-60 membrane with the highest IEC (2.11 meq·g^{-1}) had very high hydroxide ion conductivity of 131.9 mS·cm^{-1} at 80 °C, which was attributed to the well assembled nano-channels with distinct phase separation evidenced by small-angle X-ray scattering (SAXS). It was found that the hydrated QTBMs membranes were mechanically stable with moderate water uptakes and swelling ratios, high chemical stability under the harsh alkaline conditions. This work provides a facile way to prepare anion exchange membranes (AEMs) with high performances for the application in alkaline fuel cells.

Keywords Aromatic side-chain quaternary ammonium; Bromination; Alkaline anion exchange membrane; Poly(arylene ether sulfone)s

INTRODUCTION

Recently, anion exchange membrane fuel cells (AEMFCs) have aroused growing interest in power devices for the foreseeable applications. Compared to the proton exchange membranes (PEMs) fuel cells, AEMFCs can use non-precious metal-based catalysts (like sliver, cobalt, or nickel) and non-perfluorinated ionomers, which makes this kind of fuel cells more cost effective[1–3]. However, as an essential component of AEMFCs, anion exchange membrane (AEM) faces many challenges. The most important one is that the ionic conductivities of the reported AEMs are lower than that of the proton exchange membranes due to the differences in mobility between H^+ and OH^-. It is well-known that high ionic conductivity, good mechanical properties and better alkaline stabilities are the key issues to be solved before the practical application of AEMs in AEMFCs. The comprehensive properties of reported AEMs, except for alkali doped polymer AEMs, are controlled by the nature of anion conductive polymers with cationic head-groups for transporting hydroxyl anions and the backbones. The creation of anion conductive polymers with high conductivity and acceptable mechanical properties is based on the combination

* This work was financially supported by the National Natural Science Foundation of China (No. 51173045), and Student Research Program (SRP) Funds of South China University of Technology (Nos. 105612015S165 and 105612016S198).
** Corresponding author: Xiu-hua Li (李秀华), E-mail: lixiuhua@scut.edu.cn
Received December 16, 2016; Revised February 7, 2017; Accepted February 8, 2017
doi: 10.1007/s10118-017-1941-6

of alkali stable cationic head-groups and chemical stable polymeric backbones, which is one of the most dynamic research branches of AEMs.

Many kinds of AEMs have been developed by functionalizing the engineering thermoplastics. They exhibit excellent chemical and thermal stabilities and mechanical properties, such as poly(arylene ether sulfone)[4–7], poly(arylene ether ketone)[8, 9], poly(phenylene oxide)[10, 11], poly(fluorenyl ether ketone sulfone)[12, 13] *etc.* Constructing phase-separated morphologies with well-connected nano-channels for PEMs is an effective way to enhance proton conductivity[14–16]. Multiblock segments[12, 17–19] and side chain ionic groups[9, 20–22] have recently been used to improve hydroxide conductivity of AEMs by constructing nanostructures with microphase separation between hydrophilic and hydrophobic domains. However, the mechanical properties and chemical stabilities of AEMs based on the block ionomers strongly rely on the high swollen hydrophilic domains because of the nature of main-chain type ionic groups which attach closely onto the backbones of the hydrophilic segments[12, 17–19]. Side-chain type AEMs with end ionic groups in side chains have unique power to maximize the functions of polymer backbones and conductive functional groups, and avoid the interference between them by distancing the cationic centers from the polymer backbones with covalent side chains[9, 21–23]. These membranes have enhanced comprehensive properties. However, few aromatic ionomers containing side-chain end ionic groups have been reported due to the limitations of appropriate monomers and conversion approaches.

We have previously reported that using the conjugate aromatic side chains to avoid the presence of β hydrogen atoms is a promising way to alleviate the Hofmann degradation and enhance the chemical stability[20, 23]. The best performance of side-chain type AEMs shows the conductivity of 93.0 $mS \cdot cm^{-1}$ at 80 °C, which results from the fact that the upmost ion exchange capacity (IEC) of these membranes cannot broke the value of 1.68 $meq \cdot g^{-1}$ because of the configuration of monomer molecule[23]. In this work, we synthesized a new difluorodiphenyl sulfone monomer with four benzyl groups by Suzuki coupling reaction. It offered multi-positions to construct side-chain type AEMs with dense ionic groups. The quaternary ammonium groups densely anchored at the side-chain benzyl positions of the copolymers. The IEC values of the obtained AEMs were adjusted by the molar ratios of the monomers. The properties of the membranes were evaluated in terms of IEC, hydroxide conductivity, water uptake, swelling ratio, the number of bonded water per ammonium group (λ), volumetric ion exchange capacity (IEC_{Vwet}), mechanical and thermal properties, and chemical stability. This work provides a facile way for the preparation of high performance AEMs with promising applications in alkaline fuel cells.

EXPERIMENTAL

Materials

Palladium acetate was purchased from Accela ChemBio Co., Ltd., Shanghai. 4,4′-Difluorodiphenyl sulfone (DFDPS) was purchased from TCI Inc. 3,5-Dimethylphenylboronic acid, bisphenol A (BPA), triphenylphosphine were purchased from Aladdin Reagent, Shanghai, China. All the other used solvents and reagents were obtained from commercial suppliers without any purification. 3,3′-Dibromo-4,4′-difluorodiphenyl sulfone (DBDFDPS) was prepared according to the procedures reported by Li *et al*[24].

Synthesis of 3,3'-Di(3'',5''-dimethylphenyl)-4,4'-difluorodiphenylsulfone

5.562 g (13.5 mmol) of DBDFDPS, 5.062 g (33.75 mmol) of 3,5-dimethylphenylboronic acid, 11.4 g (54 mmol) of potassium phosphate, 303 mg (1.35 mmol, 10%) of palladium acetate, 708 mg (2.7 mmol) of triphenylphosphine were dissolved in 60 mL of toluene in a 250 mL Schlenk flask equipped with an electromagnetic stirrer. The reaction mixture was heated at 115 °C for 20 h under negative pressure. After then the solvent was removed by rotary evaporation to afford off-white crude product. The crude product recrystallized from ethanol twice to give a pure white crystal, a new difluoride monomer, 3,3′-di(3″,5″-dimethylphenyl)-4,4′-difluorodiphenyl sulfone (DDMPDFDPS), with a yield of 82%. ^{1}H-NMR (400 MHz, DMSO-d_6, δ): 8.13–8.15 (m, 4H), 7.59–7.61 (m, 2H), 7.48–7.50 (d, 4H), 7.34–7.35 (s, 2H), 2.37 (s, 12H).

Synthesis of Copoly(arylene ether sulfone)s Containing Tetra Benzylmethyl Groups (TBMs)

The above obtained monomer DDMPDFDPS was copolymerized with bisphenol A and 4,4′-difluorodiphenyl sulfone to produce poly(arylene ether sulfone)s containing tetra methyl groups on the ends of aromatic side-chains. The contents of DDMPDFDPS were 30 mol%, 40 mol%, 50 mol% and 60 mol% in the total difluorodiphenyl sulfone monomer loadings respectively. Target stoichiometric mixtures with 1:1 molar ratio of bisphenol to difluorodiphenyl sulfone monomers gave high molecular weight polymers *via* nucleophilic substitution polycondensations. The copolymers were named as TBM-*x*, where "*x*" represented the molar ratios of DDMPDFDPS to the total difluorodiphenyl sulfone monomers loadings. A typical polymerization procedure of TBM-30 was as follows. A 50 mL three-neck round-bottomed flask equipped with a Dean-stark trap, a nitrogen inlet/outlet, a condenser and a magnetic stirrer, was charged with DDMPDFDPS (0.6938 g, 1.5 mmol), DFDPS (0.8899 g, 3.5 mmol), bisphenol A (1.1415 g, 5 mmol), potassium carbonate (1.0350 g, 7.5 mmol), *N*,*N*′-dimethylacetamide (DMAc) (8 mL) and toluene (15 mL). The reaction was carried out at 145 °C for 4 h under nitrogen atmosphere and then toluene was distilled from the reaction mixture. After removing toluene, the reaction temperature was raised to 180 °C and kept for about 18 h. When the reaction mixture became viscous, about 30 mL of additional DMAc was added. Then the reaction mixture was poured into 300 mL of methanol containing 3 mL of concentrated HCl to form the fibrous product. The product was washed several times with deionized water and methanol, and then dried at 80 °C under vacuum for 24 h to give TBM-30 with a yield of 98.5%. All the other TBMs were obtained with the yields of *ca.* 98%.

Synthesis of Bromomethylated Poly(arylene ether sulfone)s Containing Tetra Benzylmethyl Groups (BrTBMs)

The bromomethylated polymers were named as BrTBM-*x*, where "*x*" represented the molar ratios of DDMPDFDPS to the total difluorodiphenyl sulfone monomers loadings. A typical procedure of BrTBM-30 was as follows. TBM-30 (1.00 g, the amount of $-CH_3$ was 2.36 mmol), *N*-bromosuccinimide (NBS) (0.31 g, 2.36 mmol) and azobisisobutyronitrile (AIBN) (14 mg) and 25 mL of 1,1,2,2-tetrachloroethane were added into a three-necked flask equipped with a magnetic stirrer, a nitrogen inlet and a condenser. The reaction was carried out at 80 °C for 4 h under nitrogen. The mixture was then cooled to room temperature and poured into 200 mL of methanol to precipitate out the crude brominated polymer. The precipitate was washed with methanol three times, and dried in a vacuum at 60 °C for 24 h to give BrTBM-30 with a yield of 94.5%.

Membrane Preparation

A typical procedure was as follows. 0.5 g of BrTBM-30 was dissolved in 8 mL of 1,1,2,2-tetrachloroethane, then cast onto a leveled glass plate. After dried at room temperature for 24 h, a piece of tough membrane was obtained. The membrane was immersed in 33% trimethylamine (TMA) aqueous solution at room temperature for 48 h and then washed with deionized water several times to give a quaternized membrane. The quaternized membrane was immersed in 1 $mol \cdot L^{-1}$ NaOH solution for another 48 h to obtain the OH^- form membrane QTBM-30.

Characterizations and Measurements

^{1}H-NMR, TGA, GPC, SAXS and mechanical properties

^{1}H-NMR spectra were recorded on a Bruker AVANCE 400S instrument with $CDCl_3$ or DMSO-d_6 as the solvent and tetramethylsilane (TMS) as the standard. Thermogravimetric analysis (TGA) was performed in a nitrogen atmosphere with a TAINC SDT Q600 thermogravimetric analyzer at a heating rate of 10 $K \cdot min^{-1}$. Gel permeation chromatography (GPC) analyses were measured on a Waters 510 HPLC equipped with a UV detector at 254 nm. Chloroform was used as an elution solution with the flow rate of 1 $mL \cdot min^{-1}$ and standard polystyrenes Shodex STANDARD SM-105 were used as standards. Small-angle X-ray scattering (SAXS) spectra were measured for the dry quaternized membranes at room temperature. SAXS experiments were performed on an Anton Paar SAXSess instrument with Cu Kα radiation (wavelength = 0.154 nm). The effective scattering vectors (q) were calculated from the scattering angles (θ) using the equation of $q = 4\pi\sin 2\theta/\lambda$, where λ

and 2θ were the incident wavelength and total scattering angle, respectively. The mechanical properties of membranes were measured by using an Instron M3300 Electromechanical Universal Testing Machine at a speed of 5 mm·min^{-1} at atmosphere conditions (25 °C, 100% relative humidity (RH)). The size of the sample was 50 mm × 5 mm.

Water uptake, IEC, λ, swelling ratio and IEC$_{Vwet}$

The water uptakes (WU) of the samples were defined as the increase in weight ratios of the wet membranes to the original dry membranes and calculated by the Eq. (1):

$$\mathrm{WU} = \frac{W_{\mathrm{wet}} - W_{\mathrm{dry}}}{W_{\mathrm{dry}}} \times 100\% \tag{1}$$

where W_{wet} and W_{dry} are the weight of the membranes after and before water absorption respectively.

The IECs of the membranes were determined using Mohr titrations. Approximately 0.2 g of a membrane (OH^- form) was immersed in 0.5 mol·L^{-1} HCl for 24 h and washed with water completely to give the membrane (Cl^- form). After then the membrane (Cl^- form) was immersed in 50 mL of 0.2 mol·L^{-1} $NaNO_3$ for 24 h and titrated with 0.01 mol·L^{-1} $AgNO_3$ using K_2CrO_4 as a colorimetric indicator. The IEC value of the membrane was calculated from the Eq. (2):

$$\mathrm{IEC} = \frac{M_{\mathrm{AgNO_3}} \times V_{\mathrm{AgNO_3}}}{W_{\mathrm{dry}}} \tag{2}$$

where $M_{\mathrm{AgNO_3}}$ (mol·L^{-1}) and $V_{\mathrm{AgNO_3}}$ (mL) are the concentration and consumed volume of the $AgNO_3$ solution respectively, and W_{dry} (g) is the weight of the dry membranes (Cl^- form).

λ was calculated by the following Eq. (3):

$$\lambda = \frac{\mathrm{WU}}{18.02} \times \frac{1000}{\mathrm{IEC}} \tag{3}$$

The swelling ratio (SR) of the membranes were defined as length ratios of the wet membranes to the dry membranes and calculated by the Eq. (4):

$$\mathrm{SR} = \frac{L_{\mathrm{wet}} - L_{\mathrm{dry}}}{L_{\mathrm{dry}}} \times 100\% \tag{4}$$

where L_{wet} and L_{dry} are the lengths of the membranes after and before water absorptions respectively.

Volumetric ion exchange capacity ($\mathrm{IEC_{Vwet}}$) of the wet membranes was calculated from the swelling ratios and the titrated IECs *via* the Eq. (5):

$$\mathrm{IEC_{Vwet}} = \frac{\mathrm{IEC}}{\frac{1}{\rho_{\mathrm{polymer}}} \times (1 + \mathrm{SR})^3} \times 100\% \tag{5}$$

where ρ_{polymer} is the density of dry membranes.

Hydroxide conductivity and E_a

The hydroxide conductivity (σ) of the AEMs was measured by two-probe electrochemical impedance spectroscopy (EIS) using an IviumStat frequency response analyzer as previously reported[23]. The values of hydroxide-transport-activation-energy E_a of these ionomers membranes were calculated from the Eq. (6):

$$E_a = -b \times R \tag{6}$$

where b is the slope of the regressed linear $\ln\sigma \sim 1000/T$ plots, and R is the gas constant (8.314 J·(mol·K)$^{-1}$).

RESULTS AND DISCUSSION

Monomer and Polymer Synthesis

As shown in Scheme 1, a new monomer of difluorodiphenyl sulfone with pendent multi-phenylmethyl groups, 3,3′-di(3″,5″-dimethylphenyl)-4,4′-difluorodiphenyl sulfone (DDMPDFDPS), was successfully synthesized *via* Suzuki coupling reaction from 3,3′-dibromo-4,4′-difluorodiphenyl sulfone (DBDFDPS) and 3,5-dimethylphenylboronic acid with a yield of 82% in the presence of palladium acetate and potassium phosphate. The structure of DDMPDFDPS was confirmed by ^{1}H-NMR and ^{13}C-NMR spectra (Fig. 1). The characteristic peaks of phenyl-methyl group are observed at δ = 2.32, 7.10 and 7.18. The signal at δ = 2.32 is contributed to the proton of methyl groups which are designed as high-density reaction sites for the functionalizations of quaternary ammonium groups (Fig. 1A). The carbon atoms of DDMPDFDPS are well assigned in Fig. 1(B).

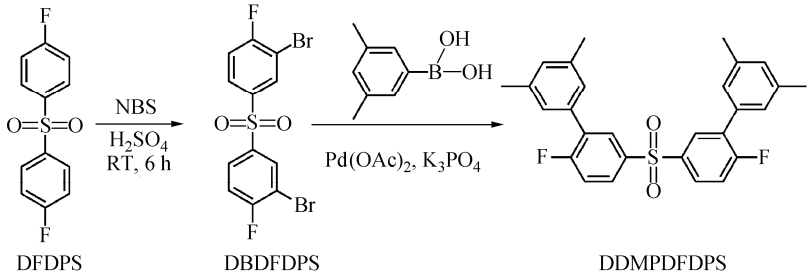

Scheme 1 Synthetic road to monomer DDMPDFDPS

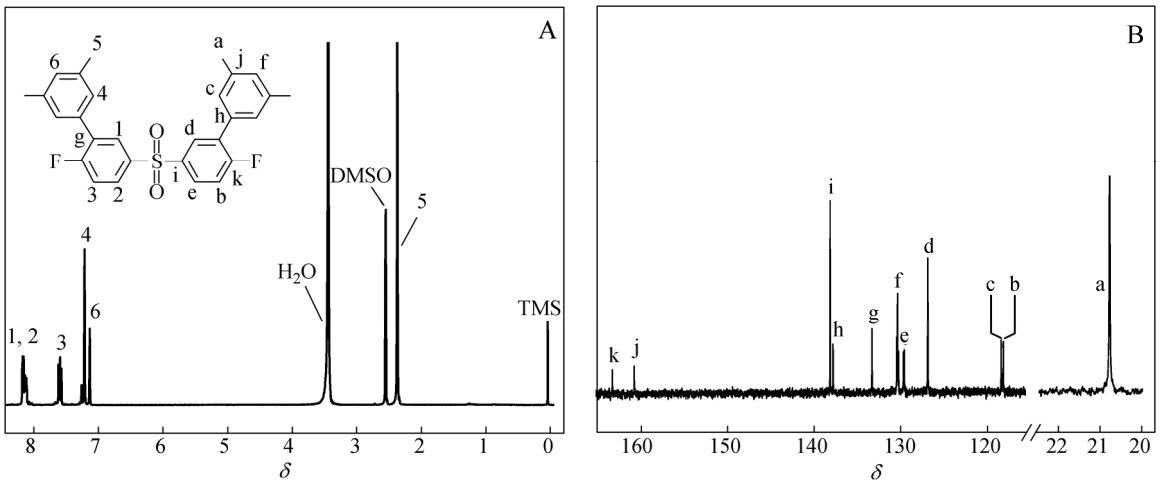

Fig. 1 ^{1}H-NMR spectrum (A) and ^{13}C-NMR spectrum (B) of DDMPDFPS

Scheme 2 shows the synthetic route to poly(arylene ether sulfone)s containing side-chain aromatic benzylmethyl quaternary ammonium groups (QTBMs) through nucleophilic substitution polycondensation, bromination, quaternization and alkalization. The GPC results of second-generation parent polymers (BrTBMs) of the ionomers are listed in Table 1. M_n and M_w of the parent polymers are both higher than 30.1 kg·mol^{-1}, indicating the high molecular weights of obtained ionomers of QTBMs.

Figure 2 shows the ^{1}H-NMR spectra of the parent polymers (TBM-30 and BrTBM-30) and the ionomer QTBM-30 in OH^- form. Compared the ^{1}H-NMR spectra of the brominated polymer and the first-generation parent polymer (Figs. 2a and 2b), a new peak 10 is found at δ = 4.45 in Fig. 2(b), which manifests that the subsequent bromination of the first generation parent polymer has been successfully conducted. The degree of the bromination (DBM) of BrTBM-30 was calculated from the integral ratio of protons of bromomethyl groups

to those of the remaining methyl groups (Fig. 2b). Other BrTBMs were obtained using the same method. All the values of the DBMs are listed in Table 2. It is obvious that the degrees of the brominations of TBMs are higher than 75%. To convert the bromomethyl groups to the quaternary ammonium groups, the BrTBMs samples were treated with trimethylamine aqueous solution. The alkalized QTBM-30 shows a new signal 11 at $\delta = 3.08$ in the ^{1}H-NMR spectrum (Fig. 2c), which is assigned to the proton of methyl groups in quaternized ammonium. The ionization of BrTBMs varies from 75% to 85%, which is higher than that of the side-chain-type AEMs in the previous report[23] owing to the ionic cluster effects.

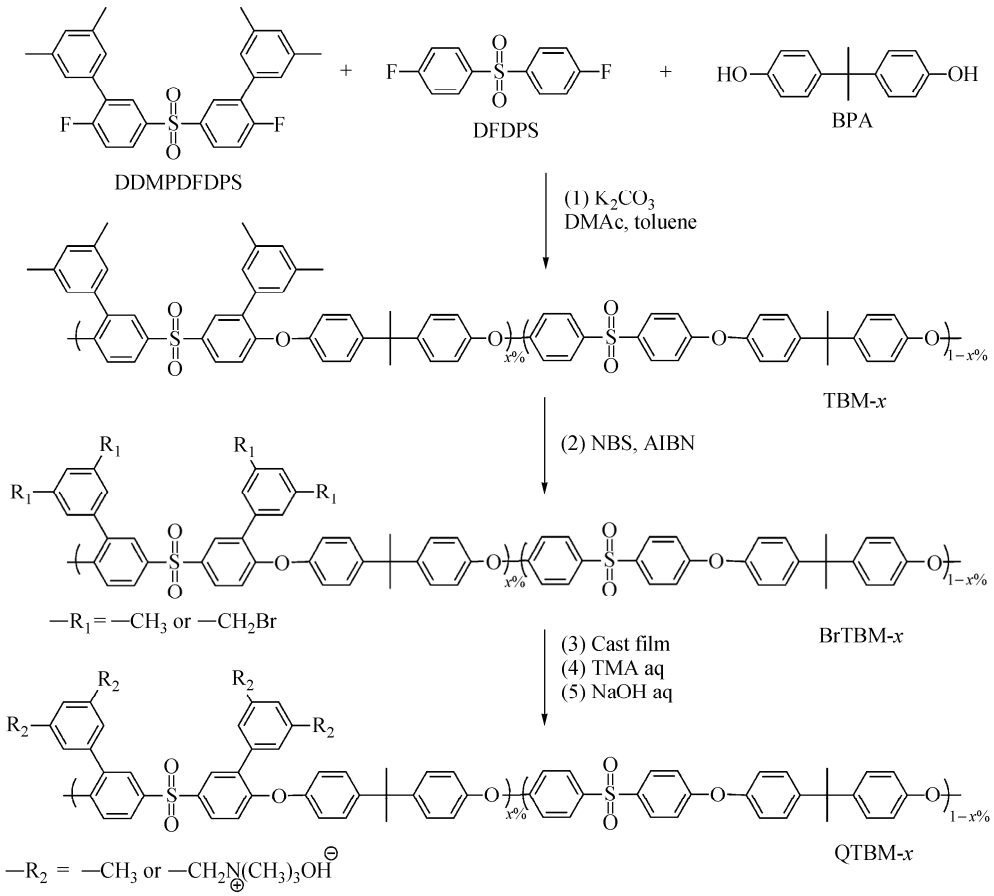

Scheme 2 Synthetic route to poly(arylene ether sulfone)s ionomers QTBMs

Table 1 Molecular weights of BrTBMs measured by GPC and the results of bromination and ionization

Sample	M_n (kg·mol^{-1})	M_w (kg·mol^{-1})	M_w/M_n	Conv. of bromination [a] (%)	Conv. of ionization [b] (%)
BrTBM-30	40.4	95.6	2.4	75.0	85.1
BrTBM-40	60.5	178.9	3.0	84.0	80.5
BrTBM-50	30.1	50.2	1.7	76.8	80.9
BrTBM-60	82.8	416.4	3.0	82.0	75.8

[a] Calculated from the ratio of experimental DBM to theoretical DBM (Experimental DBM was determined by ^{1}H-NMR; theoretical DBM was calculated from feed molar ratio of NBS/—CH_3, which is 1/1.); [b] Calculated from the ratio of experimental IEC to theoretical IEC (Experimental IEC was determined by titration; theoretical IEC was calculated from experimental values of DBM.)

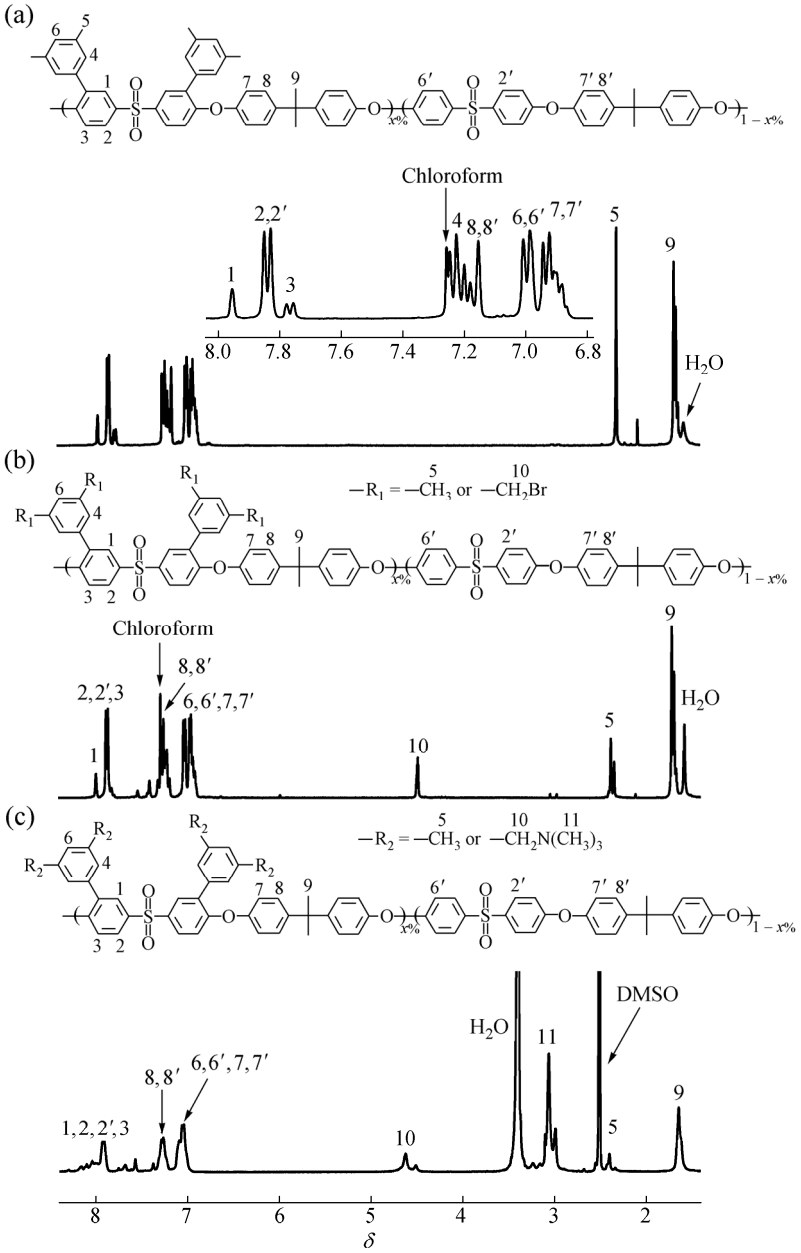

Fig. 2 ^{1}H-NMR spectra of (a) TBM-30, (b) BrTBM-30 and (c) QTBM-30

Table 2 DBM, IEC, water uptake, swelling ratio, hydroxide conductivity of QTBMs and the reported PAES-Qs and MPAES-Q-2

Membrane	DBM	IEC	WU (%)		SR (%)		σ (mS·cm^{-1})	
		(meq·g^{-1})	25 °C	80 °C	25 °C	80 °C	25 °C	80 °C
QTBM-30	3.00	1.36 ± 0.01	34.2 ± 1.2	38.8 ± 3.0	11.1 ± 0.1	13.5 ± 0.4	14.3 ± 0.2	24.7 ± 0.1
QTBM-40	3.36	1.75 ± 0.03	43.8 ± 4.7	56.8 ± 4.2	13.5 ± 0.3	19.0 ± 0.6	24.9 ± 0.0	54.4 ± 0.2
QTBM-50	3.07	1.90 ± 0.02	68.8 ± 2.7	111.5 ± 3.1	25.3 ± 0.0	42.3 ± 0.2	32.3 ± 0.1	72.9 ± 0.2
QTBM-60	3.28	2.11 ± 0.01	149.6 ± 0.8	186.7 ± 2.4	34.4 ± 0.2	47.4 ± 0.1	59.1 ± 0.2	131.9 ± 0.3
PAES-Q-90[22]	1.62	1.68 ± 0.04	60.6 ± 4.1	99.5 ± 2.7	21.2 ± 3.3	33.3 ± 1.4	39.2 ± 0.2	93.0 ± 0.2
PAES-Q-75[22]	1.33	1.49 ± 0.05	36.8 ± 2.1	59.6 ± 3.1	7.8 ± 0.4	15.6 ± 3.0	21.9 ± 0.1	47.3 ± 0.1
MPAES-Q-2[22]	1.36	1.30 ± 0.00	91.4 ± 1.5	424.9 ± 35.1	24.9 ± 2.0	50.0 ± 6.4	14.6 ± 0.1	28.1 ± 0.1

The aggregate structures of obtained AEMs were investigated by the small-angle X-ray scattering (SAXS) technique. The patterns of them are shown in Fig. 3. To highlight the effect of dense side-chain quaternary ammonium groups, side-chain type AEM PAES-Q-90 (IEC = 1.68 meq·g^{-1}) and main-chain type AEM MPAES-Q-2 (IEC = 1.30 meq·g^{-1}) with the similar backbones (Scheme 3) were also measured. Their SAXS patters are shown in Fig. 3. It is clear that the main-chain quaternary ammonium groups in MPAES-Q-2 form low degree assembly ionic clusters with a SAXS peak at 0.105 nm^{-1}, corresponding to a Bragg spacing of about 59.8 nm. Moreover, the calculated integral areas of these AEMs make it clear that the SAXS peaks of QTBMs are stronger than that of MPAES-Q-2 with q values higher than 0.107 nm^{-1}. The intensities of the SAXS peaks of QTBMs increase with the increase of IEC$_{Vwet}$ (Table 3). Among the QTBMs group, QTBM-40 has the highest IEC$_{Vwet}$ (1.28 meq·cm^{-3} at 25 °C) with obviously phase separation. PAES-Q-90 gives the strongest SAXS peak

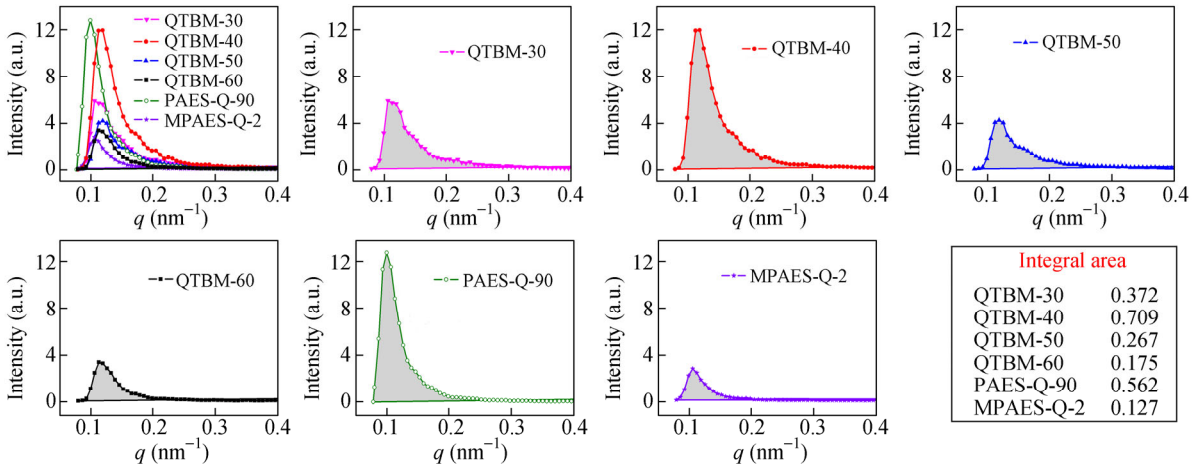

Fig. 3 SAXS patterns of QTBMs, PAES-Q-90 and MPAES-Q-2

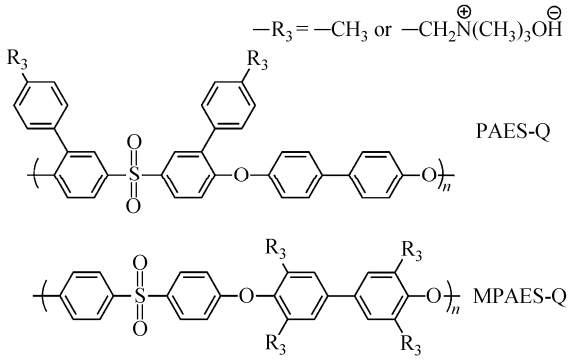

Scheme 3 Chemical structures of the reported PAES-Q and MPAES-Q-2

Table 3 λ, IEC$_{Vwet}$, σIEC$_{Vwet}$ of nano-channels of QTBMs and the reported PAES-Qs and MPAES-Q-2

Membrane	IEC (meq·g^{-1})	λ		IEC$_{Vwet}$ (meq·cm^{-3})		σIEC$_{Vwet}$ (mS·cm^{2}·meq^{-1})	
		25 °C	80 °C	25 °C	80 °C	25 °C	80 °C
QTBM-30	1.36	14.0	15.8	1.06	1.00	13.5	24.7
QTBM-40	1.75	13.9	18.0	1.28	1.11	19.4	49.0
QTBM-50	1.90	20.1	32.6	1.03	0.70	31.4	104.1
QTBM-60	2.11	39.4	49.1	0.93	0.70	63.5	188.4
PAES-Q-90[22]	1.68	20.0	32.9	1.01	0.76	38.8	122.4
PAES-Q-75[22]	1.49	13.8	22.3	1.27	1.03	17.2	45.9
MPAES-Q-2[22]	1.30	38.6	179.6	0.71	0.41	20.6	68.5

at 0.10 nm^{-1} with a Bragg spacing of 62.8 nm owing to the best continuity of the ionic groups and relatively high IEC_{Vwet} (1.01 $meq \cdot cm^{-3}$ at 25 °C).

Water Uptake, Dimensional Swelling and Hydroxide Conductivity of QTBMs

Water uptakes, swelling ratios and ion conductivities of the QTBMs membranes in hydroxide ion form were measured at different temperatures. The corresponding results are summarized in Table 2 and Figs. 4–6. As shown in Table 2, Fig. 4 and Fig. 5, water uptakes and swelling ratios of AEMs increase with the increase of temperature and IEC. The temperature dependence of water uptake and swelling ratio of the QTBMs membranes are much lower than that of the reported AEMs containing similar backbones with lower density of ionic groups[23]. In particular, compared with that of the main-chain type AEM MPAES-Q-2 (IEC = 1.30 $meq \cdot g^{-1}$), the nano-channel structures of the QTBMs membranes are more stable with temperature variation. The water uptake of the QTBMs membranes, which have higher IECs than that of MPAES-Q-2, rises from 4.6% to 42.7% at a temperature rise of 55 °C, while their swelling ratios increase from 2.4% to 17%. Whilst the water uptake and swelling ratio changes of MPAES-Q-2 are 333.5% and 25.1% respectively.

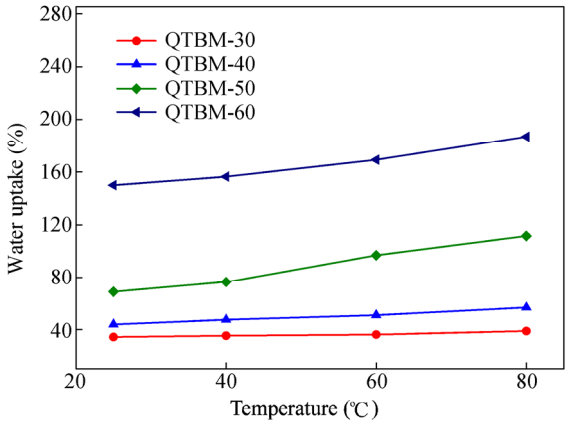

Fig. 4 Water uptakes of QTBMs at different temperature

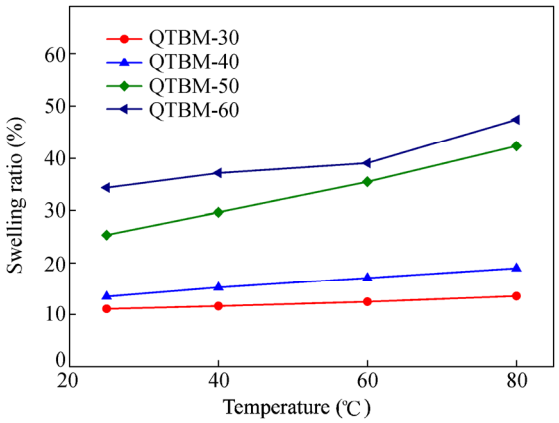

Fig. 5 Swelling ratios of QTBMs at different temperature

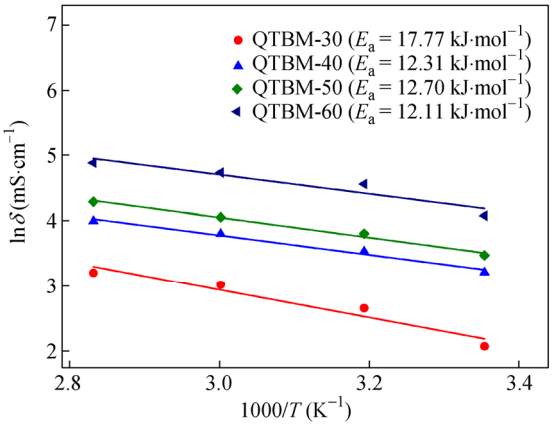

Fig. 6 The plots of lnσ *via* 1000/T of QTBMs

Since hydroxide ions can easily absorb carbon dioxide molecules in air and transform into bicarbonate ions[25], the measurement of hydroxide ion conductivity is performed in degassed water under the protection of N_2. The QTBMs membranes have the conductivities higher than 10 $mS \cdot cm^{-1}$ (Table 2), which satisfies the requirement in the ion transportation of AEMs in the fuel cells[2]. The conductivities of the QTBMs membranes increase from 14.3 $mS \cdot cm^{-1}$ to 59.1 $mS \cdot cm^{-1}$ at 25 °C, and 24.7 $mS \cdot cm^{-1}$ to 131.9 $mS \cdot cm^{-1}$ at 80 °C with

increasing IEC from 1.36 meq·g^{-1} to 2.11 meq·g^{-1}. Compared with the reported aromatic AEMs, the QTBMs membranes show very high conductivity under similar conditions. Specifically, QTBM-60 (2.11 meq·g^{-1}) exhibits hydroxide conductivities of 59.1 mS·cm^{-1} at 25 °C, and 131.9 mS·cm^{-1} at 80 °C respectively, which are much higher than those of some reported side-chain-type AEMs[22, 23, 26] and main-chain-type AEMs with nano-channels structures[12, 17]. QTBM-60 surpasses some random ionomers with much higher IEC values over 2.38 meq·g^{-1} in conductivity[13, 27, 28]. It strongly supports the micro phase separation and continuity of ionic clusters, which are important to build up high performance nano-channel structures. Table 2 also lists the conductivities of side-chain-type AEMs (PAES-Q-75 and PAES-Q-90) and main-chain-type AEM (MPAES-Q-2)[23] based on the similar backbones with lower density of functional groups. They all have ability to form nano-channels (Fig. 3). It should be pointed out that the QTBMs membranes with IEC values lower than 1.75 meq·g^{-1} have no advantage over the rivals because of the poor continuity of ionic clusters. The main-chain-type AEM MPAES-Q-2 surpasses QTBM-30 in conductivity owing to the same reason, suggesting the superiority of homopolymerization in getting ionomers with regularity structures to guarantee the continuity of the ion transportation channels. However, it can also give the copolymer ionomers with good regular structures by well adjusting the copolymerizations. QTBM-60 exhibits the nano-channels with the best continuity among the QTBMs AEMs listed in Table 2 and wins the competitions of ion transportation.

In order to explore the relationships between the structure of nano-channels and hydroxide conductivity, Table 3 lists the parameters of nano-channels of the QTBMs membranes in terms of hydration number (λ), IEC_{Vwet} and σ/IEC_{Vwet}. λ is the number of bonded water molecules per quaternary ammonium group of the ion transportation channels in hydrated membranes. IEC_{Vwet} is volumetric ion exchange capacity of hydrated membranes, which can be taken as the index of distribution of the ion transportation channels at working conditions. The value of σ/IEC_{Vwet} reflects the conductivity of per meq of quaternary ammonium groups of the ion transportation channels of the hydrated membranes. A comprehensive balance of λ and the distribution of the ion transportation channels is necessary to afford good performance of the AEMs. It is clear that λ and IEC_{Vwet} of main-chain-type AEM MPAES-Q-2 show strong temperature dependence (Table 3). The bonding water molecules around quaternary ammonium groups are necessary to build up the high way for ion transportation. However, excessive water molecules possibly break up the continuity of the ionic clusters and decrease the ion transportation capacity of the nano-channels. The coaction of dense quaternary ammonium groups enhances the water absorption and affords adequate water uptakes, moderate λ. The combination of copolymerization and end-ionization of side-chain guarantees QTBM-60 having well distribution of ion transportation channels at the investigation temperature window with high IEC_{Vwet} varying from 0.70 meq·cm^{-3} to 0.93 meq·cm^{-3}. QTBM-60 shows the most effective high way for ion transportation with the highest values of σ/IEC_{Vwet} (63.5 mS·cm^2·meq^{-1} at 25 °C and 188.4 mS·cm^2·meq^{-1} at 80 °C respectively).

Hydroxide conductivities of the QTBMs membranes increase as a function of temperature (Fig. 6). It is obvious that the relationship between $\ln\sigma$ and $1000/T$ follows Arrhenius behavior. The calculated hydroxide-transport-activation-energies E_a of the QTBMs membranes varied from 17.77 kJ·mol^{-1} to 12.11 kJ·mol^{-1}. All the other QTBMs membranes, except QTBM-30, have E_a around 12.31 kJ·mol^{-1}, which are close to that of Nafion-117 (12.75 kJ·mol^{-1})[29]. It is obvious that the temperature dependence of hydroxide ion mobility in the QTBMs membranes (the DDMPDFPS feed ratios higher than 30%) is low. Especially, QTBM-60 with E_a value of 12.11 kJ·mol^{-1} shows the lowest temperature sensibility in conductivity resulting from the best continuity of nano-channels.

Mechanical Properties, Thermal Properties and Alkaline Stability

The mechanical properties of the QTBMs membranes are shown in Table 4. It is obvious that the mechanical properties of the QTBMs membranes decrease sharply with an increase of IEC owing to the enhanced plasticization of the multiplied water uptakes. However, these membranes display values of tensile strength of 5.8–25.6 MPa, tensile modulus of 51.4–913.5 MPa, and elongation at break of 32.2%–66.4%. These results indicate that the QTBMs membranes are robust for the fabrication of membrane electrode assembly for AEMFCs.

Table 4 Mechanical properties of QTBMs membranes

Sample	IEC [a] (meq·g^{-1})	Tensile strength [b] (MPa)	Tensile modulus [b] (MPa)	Elongation at break [b] (%)
QTBM-30	1.36 ± 0.01	25.6 ± 1.1	913.5 ± 19.9	32.2 ± 2.4
QTBM-40	1.75 ± 0.03	15.4 ± 3.6	280.7 ± 32.7	44.7 ± 4.1
QTBM-50	1.90 ± 0.02	11.5 ± 3.0	123.1 ± 11.8	66.4 ± 4.4
QTBM-60	2.11 ± 0.01	5.8 ± 1.4	51.4 ± 12.5	48.1 ± 3.7

[a] Experimental IEC, determined by titration; [b] The samples were measured at 25 °C, 100% RH.

The TGA curves of TBM-30, BrTBM-30 and QTBM-30 are shown in Fig. 7. The first step of degradation of TBM-30 is the leaving of methyl groups in the side chains, which has the maximum speed at 215 °C. The second-generation parent polymer BrTBM-30 gives three stages of weight loss. The first stage of BrTBM-30 starts at 150 °C, which is contributed to the leaving of bromides of dense and high active benzyl bromide groups. The second and third stages of weight losses are ascribed to the decomposition of the residual of first stage and polymer backbone, respectively. The decomposition behavior of QTBM-30 shows three steps process. The first stage is attributed to loosely bonding water molecules such as the absorbed surface water, and the second stage is assigned to the degradation of the quaternary ammonium groups. The third stage of weight loss is ascribed to the decomposition of the polymer backbone. Especially the degradation of the quaternary ammonium groups (maximum speed of degradation at 289 °C) lags nearly 90 °C compared with that of PAES-Q-90 (maximum speed of degradation at 200 °C)[23]. It is a side-chain type ionomer with better short-term thermal stability than the main chain type ionomer[23]. It can be seen that QTBM-30 displays much better short-term thermal stability than that of some reported ionomers.

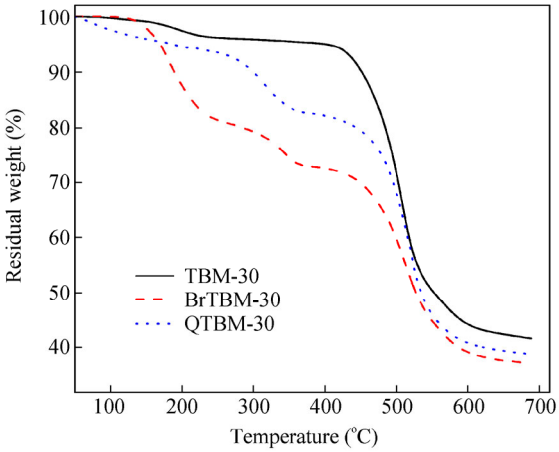

Fig. 7 TGA curves of TBM-30, BrTBM-30 and QTBM-30

The long-term durability of the QTBMs membranes in hot water at 80 °C for 500 h was further investigated in terms of IEC (Table 5). The QTBMs membranes retain their toughness and flexibility after 500 h of testing. The IEC values are higher than 92% of the initial IECs (Table 5). The high durability of the QTBMs membranes is suitable for the application in alkaline fuel cells.

The chemical stability of AEMs is one of the major challenges for the practical application of alkaline fuel cells[30]. The degradation of quaternary ammonium functionalized ionomers occurs probably *via* direct nucleophilic substitution and Hoffmann elimination under strong basic condition[2, 7, 31]. To further evaluate the chemical stability of ionomers membranes under strong basic condition, the membrane QTBM-40 was treated with 1 mol·L^{-1} NaOH solution at 60 °C for 1000 h. ^{1}H-NMR spectra of QTBM-40 are shown in Fig. 8 to manifest the changes in the ionomer structure before and after the treatment. The ^{1}H-NMR results show the relative intensities of peak 11 (—N(CH$_3$)$_3$) and peak 10 (—CH$_2$N) to peak 9 (—C(CH$_3$)$_2$—), which belongs to

Table 5 Changes in IEC and mechanical properties of QTBMs membranes after treatment with hot water at 80 °C for 500 h or 1 mol·L^{-1} NaOH solution at 60 °C for 1000 h

Sample	IEC [a] (meq·g^{-1})	Tensile strength [b] (MPa)	Elongation at break [b] (%)	Decrease amplitude (%)		
				IEC [a]	Tensile strength [b]	Elongation at break [b]
QTBM-30	1.31 ± 0.03	23.5 ± 2.1	29.2 ± 2.4	3.7	8.2	9.3
QTBM-40	1.65 ± 0.02	13.2 ± 3.5	37.9 ± 4.0	5.3	14.3	15.2
QTBM-50	1.77 ± 0.01	9.5 ± 2.7	54.4 ± 4.2	6.8	17.4	18.1
QTBM-60	1.94 ± 0.02	4.7 ± 1.0	39.2 ± 3.4	8.0	19.0	18.5

[a] Experimental IEC after treatment with hot water at 80 °C for 500 h, determined by titration; [b] The samples were measured at 25 °C, 100% RH after treatment with 1 mol·L^{-1} NaOH solution at 60 °C for 1000 h.

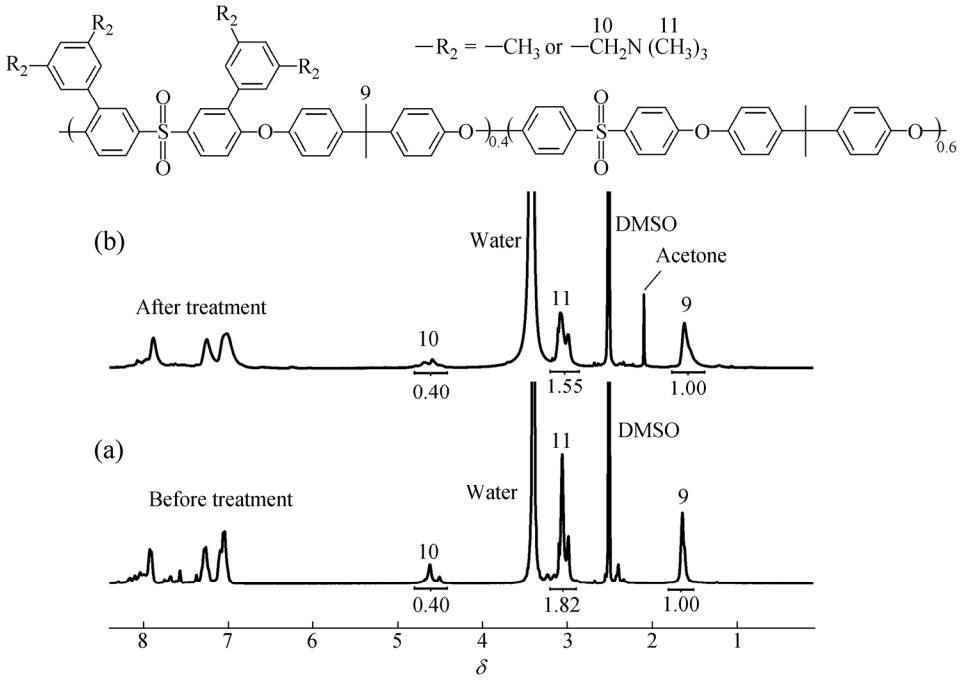

Fig. 8 ^{1}H-NMR spectra of QTBM-40 before (a) and after (b) 1 mol·L^{-1} NaOH treatment under the condition of 60 °C for 1000 h

BPA units and is stable because of the isolation from the ionic groups. The relative ratio of peak 10 to peak 9 shows no change after the test, indicating no degradation of the backbone. The relative ratio of peak 11 to peak 10 decreases resulting from the leaving group of $-N(CH_3)_3$, possibly caused by direct nucleophilic substitution. The dense ionic groups facilitate to form high performance nano-channels and trap more hydroxides inside the channels, which favors the nucleophilic substitution. However, QTBM-40 remains 86.1% of the quaternary ammonium groups after being conditioned with 1 mol·L^{-1} NaOH at 60 °C for 1000 h. Furthermore, the present membrane exhibits comparable alkaline stability to some advanced AEMs reported in the literature recently. The comb shaped PES-B100-C16 membrane maintained about 70% of the initial ionic conductivity after being soaked in 2 mol·L^{-1} NaOH at 60 °C for 360 h, which had a stability factor of large β-alkyl side chains with high electron density[32]. Dual-cation comb-shaped C18BQAPPO-3 membrane retained 80.7% of its initial hydroxide conductivity after being immersed in 1 mol·L^{-1} KOH at 60 °C for 380 h[33]. The side chain type PAES-15-IMPPO bearing pendent imidazolium-functionalized poly(phenylene oxide) (IEC = 2.55 meq·g^{-1}, OH^- form) kept 45% of the origin ionic groups after being conditioned in a 1 mol·L^{-1} KOH solution at 80 °C for 600 h[34]. Even at the end of the treatment, the treated samples present no obvious change in appearance and retain higher than 80% of the origin mechanical properties (Table 5), which also supports that the backbone of side-chain type AEMs can withstand the harsh alkaline working conditions of AEMFCs.

CONCLUSIONS

A series of hydroxide conductive QTBMs AEMs has been successfully synthesized from a new monomer and commercially available chemicals, which possess dense quaternary ammonium groups in aromatic side-chains of the poly (arylene ether sulfone)s, and with IECs ranging from 1.02 meq·g^{-1} to 2.11 meq·g^{-1}. The new monomer has conjugated aromatic side branches obtained by Suzuki coupling reaction. The dense aromatic side-chain quaternary ammonium groups in the ionomers form assembled nano-channels with varying regularity and continuity, which strongly controls the performances of the obtained anion exchange membranes. The results of SAXS and properties measurements show that the ionic clusters in QTBM-60 (IEC = 2.11 meq·g^{-1}) have assembled well-defined nano-channels with a Bragg spacing of about 56.6 nm and good continuity of high IEC_{Vwet}s at the testing conditions. QTBM-60 membrane has obvious nano-channels and shows the highest hydroxide ion conductivity of 131.9 mS·cm^{-1} at 80 °C. The properties of the hydrated QTBMs membranes display less temperature dependence, indicating the good working performances. Long-term stability test over 1000 h shows that QTBM-40 keeps 86.1% of the quaternary ammonium groups and all the treated membranes retain higher than 80% of the origin mechanical properties under the harsh alkaline conditions. This work provides a facile way to afford the side-chain ion clusters for the high performances AEMs.

REFERENCES

1 Varcoe, J.R. and Slade, R.C.T., Fuel Cells, 2005, 5: 187
2 Merle, G., Wessling, M. and Nijmeijer, K., J. Membr. Sci., 2011, 377: 1
3 Wang, Y.J., Qiao, J., Baker, R. and Zhang, J., Chem. Soc. Rev., 2013, 42: 5768
4 Li, X., Tao, J., Nie, G., Wang, L., Li, L. and Liao, S., RSC Adv., 2014, 4: 41398
5 Wang, J., Wang, J., Li, S. and Zhang, S., J. Membr. Sci., 2011, 368: 246
6 Lin, B.C., Qiu, L.H., Qiu, B., Peng, Y. and Yan, F., Macromolecules, 2011, 44: 9642
7 Zhang, Q., Zhang, Q., Wang, J., Zhang, S. and Li, S., Polymer, 2010, 51: 5407
8 Chen, D. and Hickner, M.A., Macromolecules, 2013, 46: 9270
9 Xu, S., Zhang, G., Zhang, Y., Zhao, C.J., Ma, W.J., Sun, H.C., Zhang, N., Zhang, L.Y., Jiang, H. and Na, H., J. Power Sources, 2012, 209: 228
10 Li, Q., Liu, L., Miao, Q., Jin, B. and Bai, R., Chem. Commun., 2014, 50: 2791
11 Lin, B., Dong, H., Li, Y., Si, Z., Gu, F. and Yan, F. Chem. Mater., 2013, 25: 1858
12 Li, X.H., Yu, Y.F., Liu, Q.F. and Meng, Y.Z., J. Membr. Sci., 2013, 436: 202
13 Li, X.H., Liu, Q.F., Yu, Y.F. and Meng, Y.Z., J. Mater. Chem. A, 2013, 1: 4324
14 Li, N., Wang, C., Lee, S.Y., Park, C.H., Lee, Y.M. and Guiver, M.D., Angew. Chem. Int. Ed., 2011, 123: 9324
15 Lafitte, B. and Jannasch, P., Adv. Funct. Mater., 2007, 17: 2823
16 Wang, L.M., Zhang, Q.F. and Zhang, S.B., Chinese J. Polym. Sci., 2015, 33(9): 1225
17 Li, X., Liu, Q., Yu, Y. and Meng, Y., J. Membr. Sci., 2014, 467: 1
18 Tanaka, M., Fukasawa, K., Nishino, E., Yamaguchi, S., Yamada, K., Tanaka, H., Bae, B., Miyatake, K. and Watanabe, M., J. Am. Chem. Soc., 2011, 133: 10646
19 Yokota, N., Ono, H., Miyake, J., Nishino, E., Asazawa, K., Watanabe, M. and Miyatake, K., ACS Appl. Mater. Interfaces, 2014, 6: 17044
20 Nie, G.H., Li, X.H., Tao, J.X., Wu, W.J. and Liao, S.J., J. Membr. Sci., 2015, 474: 187
21 Liu, Z., Li, X.B., Shen, K.Z., Feng, P.J., Zhang, Y.N., Xu, X., Hu, W., Jiang, Z.H., Liu, B.J. and Guiver, M.D., J. Mater. Chem. A, 2013, 1: 6481
22 Li, N., Zhang, Q., Wang, C., Lee, Y.M. and Guiver, M.D., Macromolecules, 2012, 45: 2411
23 Li, X., Nie, G., Tao, J., Wu, W., Wang, L. and Liao, S., ACS Appl. Mater. Interfaces, 2014, 6: 7585

24 Li, N., Shin, D.W., Hwang, D.S., Lee, Y.M. and Guiver, M.D., Macromolecules, 2010, 43: 9810
25 Yan, J. and Hickner, M.A., Macromolecules, 2010, 43: 2349
26 Wang, C.Y., Shen, B., Xu, C., Zhao, X.Y. and Li, J., J. Membr. Sci., 2015, 492: 281
27 Tanaka, M., Koike, M., Miyatake, K. and Watanabe, M., Polym. Chem.-UK, 2011, 2: 99
28 Li, X., Yu, Y., Liu, Q. and Meng, Y., ACS Appl. Mater. Interfaces, 2012, 4: 3627
29 Lin, B., Qiu, L., Lu, J. and Yan, F., Chem. Mater., 2010, 22: 6718
30 Hickner, M.A., Herring, A.M. and Coughlin, E.B., J. Polym. Sci., Part B: Polym. Phys., 2013, 51: 1727
31 Couture, G., Alaaeddine, A., Boschet, F. and Ameduri, B., Prog. Polym. Sci., 2011, 36: 1521
32 Lin, C.X., Zhuo, Y.Z., Lai, A.N., Zhang, Q.G., Zhu, A.M. and Liu, Q.L., RSC Adv., 2016, 6: 17269
33 He, Y., Si, J., Wu, L., Chen, S., Zhu, Y., Pan, J., Ge, X., Yang, Z. and Xu, T., J. Membr. Sci., 2016, 515: 189
34 Lin, C.X., Zhuo, Y.Z., Lai, A.N., Zhang, Q.G., Zhu, A.M., Ye, M.L. and Liu, Q.L., J. Membr. Sci., 2016, 513: 206